



# Angewandte GDCh Chemie

Eine Zeitschrift der Gesellschaft Deutscher Chemiker

[www.angewandte.de](http://www.angewandte.de)

## Akzeptierter Artikel

**Titel:** How Water Accelerates Bivalent Ion Diffusion

**Autoren:** Fei Wang, Wei Sun, Zulipiya Shadikez, Enyuan Hu, Xiao Ji, Tao Gao, Xiao-Qing Yang, Kang Xu, and Chunsheng Wang

Dieser Beitrag wurde nach Begutachtung und Überarbeitung sofort als "akzeptierter Artikel" (Accepted Article; AA) publiziert und kann unter Angabe der unten stehenden Digitalobjekt-Identifizierungsnummer (DOI) zitiert werden. Die deutsche Übersetzung wird gemeinsam mit der endgültigen englischen Fassung erscheinen. Die endgültige englische Fassung (Version of Record) wird ehestmöglich nach dem Redigieren und einem Korrekturgang als Early-View-Beitrag erscheinen und kann sich naturgemäß von der AA-Fassung unterscheiden. Leser sollten daher die endgültige Fassung, sobald sie veröffentlicht ist, verwenden. Für die AA-Fassung trägt der Autor die alleinige Verantwortung.

**Zitierweise:** *Angew. Chem. Int. Ed.* 10.1002/anie.201806748  
*Angew. Chem.* 10.1002/ange.201806748

**Link zur VoR:** <http://dx.doi.org/10.1002/anie.201806748>  
<http://dx.doi.org/10.1002/ange.201806748>

## How Water Accelerates Bivalent Ion Diffusion

Fei Wang,<sup>[a],[b]</sup> Wei Sun,<sup>[a]</sup> Zulpiya Shadike,<sup>[c]</sup> Enyuan Hu,<sup>[c]</sup> Xiao Ji,<sup>[a]</sup> Tao Gao,<sup>[a]</sup> Xiao-Qing Yang,<sup>[c]</sup> Kang Xu\*<sup>[b]</sup> and Chunsheng Wang\*<sup>[a],[d]</sup>

**Abstract:** Multivalent (MV) ion batteries (Mg, Zn, Al, etc) are considered promising alternatives to the Li-ion batteries (LIBs), while their applications suffer from the sluggish MV cation diffusion in electrolytes, electrodes, and the interfaces in between, induced by its strong electrostatic interaction with both solvent molecules and host lattices. Recent reports demonstrated that the presence of H<sub>2</sub>O molecules in the electrolyte and/or electrode significantly alleviates these MV cation diffusion barriers, but the rationales varied, and the underneath mechanism remains uncertain. In this work, we systemically investigated the effect of H<sub>2</sub>O in electrolyte and in electrode lattice on the thermodynamics and kinetics of reversible MV-ion intercalation chemistry based on a model platform of layered VOPO<sub>4</sub>. We found that H<sub>2</sub>O presence at the electrolyte/electrode interface plays the key role in assisting Zn<sup>2+</sup> diffusion from electrolyte to the surface, while H<sub>2</sub>O in the lattice structure alters the working potential. More importantly, a dynamic equilibrium between bulk electrode and electrolyte is eventually reached for the H<sub>2</sub>O transports during the charge/discharge cycles, with the water activity serving as the key parameter determining the direction of water movement and the cycling stability.

Lithium-ion batteries (LIB) satisfy most of our daily digital and mobile energy needs<sup>[1]</sup>, however, their energy limits are set by the intercalation chemistry nature. Aggressive engineering to maximize energy density have brought safety concerns<sup>[2]</sup>. As alternatives, multivalent (MV) ion batteries (Mg, Zn, Al, etc) have attracted increasing attentions for their comparable or even superior capacities to that of LIB but much lower cost<sup>[3]</sup>. However, the MV ion batteries typically suffer from the sluggish kinetics, no matter in crystalline solids, in bulk electrolytes or across the interfaces/interphases. The stronger electrostatic interaction between the MV cations and their environment constitutes the following fundamental difficulties: (1) The high energy barriers for

the diffusion within the solid electrodes, (2) The much bulkier and clumsier solvation spheres in electrolyte due to the higher solvation numbers (~6) than mono-valent cations, and (3) The especially difficult desolvation at the electrode/electrolyte interfaces. Mitigation or elimination of these barriers thus become the key to unlock these potential battery chemistries.

Recent reports demonstrated that the H<sub>2</sub>O molecules in the electrolyte and/or electrode could significantly alleviate these MV cation diffusion barriers<sup>[4]</sup>, but rationales varied. Some believed that H<sub>2</sub>O in lattice structure helps open up the diffusion tunnels, or acts as electrostatic shield for MV cations<sup>[5]</sup> <sup>[3b, 4a]</sup>, while others argued that water molecules move with the MV cations<sup>[6]</sup>. Overall, the underneath mechanism remains uncertain, mainly because of the limited analytical tools that can precisely identify how water distribute in a MV electrode/electrolyte system<sup>[7]</sup>, as well as the limited host materials that could allow reversible MV-ion insertion. This absence of fundamental understanding prevents us from further exploiting this advantage brought by water and making MV ion batteries successful.

Among the MV ion chemistries, Zn is of particular interest for its high volumetric capacities (5851 mAh cm<sup>-3</sup>), high abundance, and good compatibility with aqueous electrolytes<sup>[8]</sup>. Differing from the complications arising from interphase formation on Mg surface at the low potential, Zn resides within the electrochemical stability windows of most non-aqueous (and even aqueous) electrolytes, where facile Zn stripping/plating occurs with high reversibility<sup>[6, 9]</sup>. Thus, Zn chemistry should serve as an ideal platform to investigate how water influence the diffusion of a MV cation.

Herein, we demonstrate layered VOPO<sub>4</sub> and its hydrates as such model platforms, which could be utilized as Zn<sup>2+</sup> host in both aqueous and non-aqueous electrolytes. Using electroanalytical technologies, X-ray diffraction (XRD), neutron diffraction (ND) and the first-principle calculations, we systemically investigated the effect of H<sub>2</sub>O that exists in electrolyte and in lattice on the thermodynamics and kinetics of reversible Zn<sup>2+</sup>-ion chemistry. We found that the H<sub>2</sub>O at the electrolyte/electrode interface accelerates Zn<sup>2+</sup> diffusion from electrolyte to the bulk surface, while H<sub>2</sub>O in the bulk electrode alters the working potential. A dynamic equilibrium between bulk electrode and electrolyte is eventually reached for the H<sub>2</sub>O transports during the cycles, with the water activity ( $a_{\text{H}_2\text{O}}$ ) as the key parameter determining the

[a] Dr. F. Wang, Dr. W. Sun, X. Ji, Dr.T. Gao and Prof. C. Wang  
Department of Chemical and Biomolecular Engineering, University of Maryland College Park, MD 20740 (USA)  
E-mail: cswang@umd.edu

[b] Dr. F.Wang, Dr. K.Xu. Electrochemistry Branch, Sensor and Electron Devices Directorate, Power and Energy Division, U.S. Army Research Laboratory, Adelphi, MD 20783, USA.  
E-mail: conrad.k.xu.civ@mail.mil

[c] Dr. Z. Shadike, Dr.E.Hu, Dr. XQ. Yang. Chemistry Division, Brookhaven National Laboratory, Upton, NY 11973, USA

[d] Prof. C. Wang Department of Chemistry and Biochemistry, University of Maryland College Park, MD 20740 (USA)

Supporting information for this article is given via a link at the end of the document

## COMMUNICATION

direction of H<sub>2</sub>O movement. The mechanistic understanding about how H<sub>2</sub>O affects the transport of MV cations from electrode to electrolyte constitutes a solid foundation for the design of future MV ion batteries.

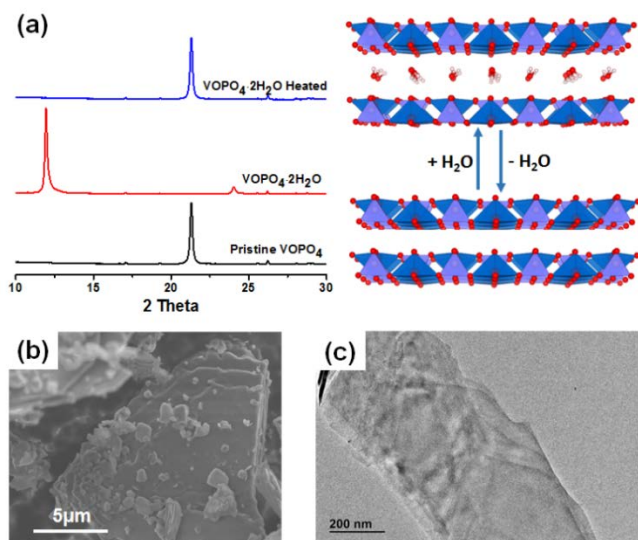


**Figure 1.** (a) XRD patterns of pristine VOPO<sub>4</sub>, VOPO<sub>4</sub>·2H<sub>2</sub>O and VOPO<sub>4</sub>·2H<sub>2</sub>O after heat treatment. The schematic illustration shows the transformation between VOPO<sub>4</sub> and VOPO<sub>4</sub>·2H<sub>2</sub>O. (b) SEM and (c) TEM image of the VOPO<sub>4</sub>.

Layered VOPO<sub>4</sub> has been used as host for monovalent-ions<sup>[10]</sup>, but, to our best knowledge, was never reported for MV cations. VOPO<sub>4</sub> has a typical (001) peak at ~21.5°, corresponding to a *d* value of 4.2 Å<sup>[11]</sup>, while the intercalation of H<sub>2</sub>O molecules into the interlayer significantly expanded basal spacing to 7.4 Å, thus pushing the peak to ~11.9° for hydrated VOPO<sub>4</sub>·2H<sub>2</sub>O<sup>[12]</sup>. The thermogravimetric analysis (Figure S1) proved that the hydration-dehydration of VOPO<sub>4</sub> is reversible, because after being heated to 500 °C, the peak of VOPO<sub>4</sub>·2H<sub>2</sub>O shifted back. VOPO<sub>4</sub> displays thin platelets with a lateral size of ~20 μm (Figure 1b), while TEM image reveals VOPO<sub>4</sub> as individual and freestanding nanosheets (Figure 1c).

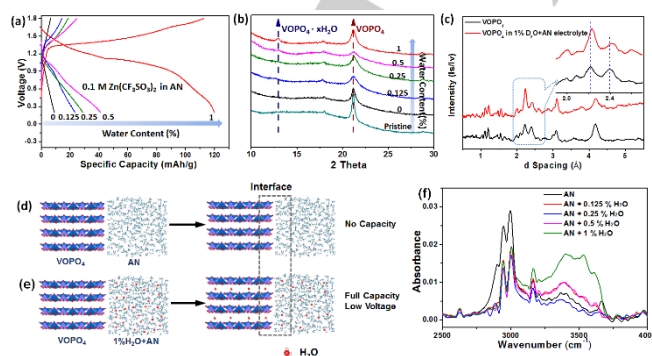


**Figure 2.** (a) The voltage profile of VOPO<sub>4</sub> between 0.2 V and 1.9 V in the 0.1 M Zn(OTf)<sub>2</sub>-AN with different water contents at 20 mA/g. (b) The XRD patterns of the VOPO<sub>4</sub> soaked in the different electrolytes for 24 hours. (c) The neutron

diffraction results of VOPO<sub>4</sub> soaked in 0.1 M Zn(OTf)<sub>2</sub>-AN with 1% D<sub>2</sub>O. The schematic illustrations of VOPO<sub>4</sub> in the 0.1 M Zn(OTf)<sub>2</sub>-AN (d) without water and (e) with 1% H<sub>2</sub>O. (f) The progression of FTIR spectra between 2500 and 4000 cm<sup>-1</sup> with water contents.

0.1 M Zn(OTf)<sub>2</sub> in acetonitrile (AN) was chosen as the base electrolyte, into which different amount of H<sub>2</sub>O was added. Only negligible capacity can be accessed from VOPO<sub>4</sub> in the water-free electrolyte (Figure 2a), while slight increase in capacity (47 mAh/g) was obtained at 0.5% H<sub>2</sub>O, followed by a rapid increase to 122 mAh/g when H<sub>2</sub>O increases to 1%. The significant increase is induced by the presence of H<sub>2</sub>O diffusion into VOPO<sub>4</sub>, as evidenced by the shift of XRD patterns (Figure 2b). EDX mapping confirms that the capacity arise from the Zn-ion intercalation (Figure S2). When dry VOPO<sub>4</sub> electrode was immersed in 0.1 M Zn(OTf)<sub>2</sub>-AN electrolytes with H<sub>2</sub>O contents below 0.5%, no significant shift in XRD peaks was observed; while a small peak representing hydrate VOPO<sub>4</sub> appeared after being exposed to 1% H<sub>2</sub>O. This difference strongly suggests that H<sub>2</sub>O intercalated into the lattice of VOPO<sub>4</sub>, and led to the capacity hike. The chemical intercalation of H<sub>2</sub>O into VOPO<sub>4</sub> can also be confirmed by ND (Figure 2c), where peak shifts to a high *d*-spacing after soaking in electrolyte containing 1% H<sub>2</sub>O, reminiscent of solid-solution behavior. The hydration of VOPO<sub>4</sub> can also be revealed by the atomic pair distribution function (PDF) technique using neutron scattering (Figure S3). Therefore, as schematically illustrated in Figure 2d and 2e, H<sub>2</sub>O migrates from water-containing electrolyte into the VOPO<sub>4</sub> lattice, and simultaneously creates a “wet interface” that assists the Zn<sup>2+</sup> intercalation, whereas a dry interface accepts the Zn<sup>2+</sup> with significant resistance (see the dotted box).

To understand why H<sub>2</sub>O migrates into VOPO<sub>4</sub>, the chemical environment of H<sub>2</sub>O molecules in 0.1 M Zn(OTf)<sub>2</sub>-AN electrolyte was investigated by FTIR (Figure 2f). When H<sub>2</sub>O-content crossed the threshold between 0.5%~1%, a strong absorption abruptly appeared at 3550 cm<sup>-1</sup> with a shoulder at ~3410 cm<sup>-1</sup>, which have been indexed to the aggregated H<sub>2</sub>O molecules<sup>[13]</sup>. In other words, at 1% H<sub>2</sub>O-content, there are suddenly “free” H<sub>2</sub>O-molecules available that neither coordinate with salt cation/anion nor the organic molecule. Upon contact with anhydrate VOPO<sub>4</sub>, they are thermodynamically driven into the lattice.

## COMMUNICATION

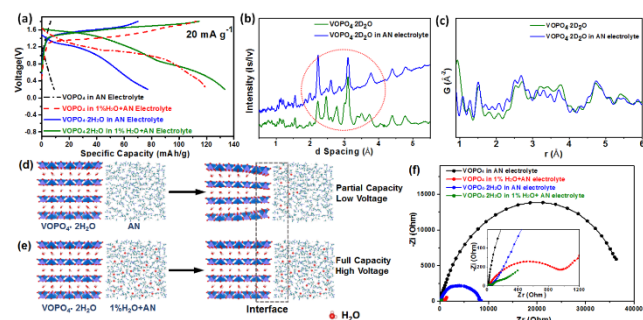


**Figure 3.** (a) The voltage profile of VOPO<sub>4</sub>·2H<sub>2</sub>O between 0.2 V and 1.9 V in the 0.1 M Zn(OTf)<sub>2</sub>-AN with different water contents at 20 mA/g. (b) The neutron diffraction and (c) the PDF refinement of neutron scattering of the VOPO<sub>4</sub>·2H<sub>2</sub>O equilibrated with anhydrous electrolytes for 24 hours. The scheme of VOPO<sub>4</sub>·2H<sub>2</sub>O in the 0.1 M Zn(OTf)<sub>2</sub>-AN (d) without water and (e) with 1% H<sub>2</sub>O. (f) EIS results of VOPO<sub>4</sub> and VOPO<sub>4</sub>·2H<sub>2</sub>O in different electrolytes.

One wonders whether the migration of H<sub>2</sub>O molecules could also happen when hydrated VOPO<sub>4</sub>·2H<sub>2</sub>O meets water-free electrolyte, where residual H<sub>2</sub>O in VOPO<sub>4</sub> lattice serves as the source of hydration for the electrolyte/electrode interface. Indeed, a higher capacity of ~135 mAh/g was delivered by the VOPO<sub>4</sub>·2H<sub>2</sub>O in electrolyte containing 1% H<sub>2</sub>O than that (122 mAh/g) of the dry VOPO<sub>4</sub> (Figure 3a). Furthermore, crystal H<sub>2</sub>O in lattice also shifts Zn<sup>2+</sup>-insertion potential higher, consistent with previous reports<sup>[4e, 5]</sup>. In strong contrast, VOPO<sub>4</sub>·2H<sub>2</sub>O in anhydrous electrolyte only delivered ~60% of that in the wet electrolyte. As shown in Figure 3b, after equilibrating VOPO<sub>4</sub>·2H<sub>2</sub>O with anhydrous electrolyte for 24 hours, a new set of diffraction peaks arose, indicating a two-phase transformation, which is also revealed by XRD (Figure S4). PDF analysis revealed a decrease in O-H bond intensity ( $r=1\text{\AA}$ ) due to the partial dehydration of VOPO<sub>4</sub><sup>[14]</sup>. A schematic illustration is thus constructed (Figure 3d and 3e), which visually depicts the water exchange between VOPO<sub>4</sub>·2H<sub>2</sub>O and electrolytes. The extraction of H<sub>2</sub>O by the anhydrous electrolyte from the interfacial region of VOPO<sub>4</sub>·2H<sub>2</sub>O leads to a poorly hydrated interface, which disfavors the Zn<sup>2+</sup> diffusion.

Since full cell kinetics are determined by the cathode (Figure S5), the charge-transfer resistances ( $R_{CT}$ ) at the cathode–electrolyte interface, as represented in EIS<sup>[15]</sup> using three-electrode cells, are much higher in the anhydrous electrolytes, while a hydrated electrode VOPO<sub>4</sub>·2H<sub>2</sub>O effectively decreases the resistance (Figure 3f). The minimum in  $R_{CT}$  occurs only when H<sub>2</sub>O is present in both electrolyte and electrode lattice, confirming that H<sub>2</sub>O dictates the Zn-ion diffusion. In the optimum scenario, the presence of H<sub>2</sub>O in both bulk electrolyte and electrode lattice would create a continuous and fully hydrated ionic passage with

little energetic barriers, significantly benefiting the Zn<sup>2+</sup> desolvation process that would be otherwise rather difficult<sup>[16]</sup>.

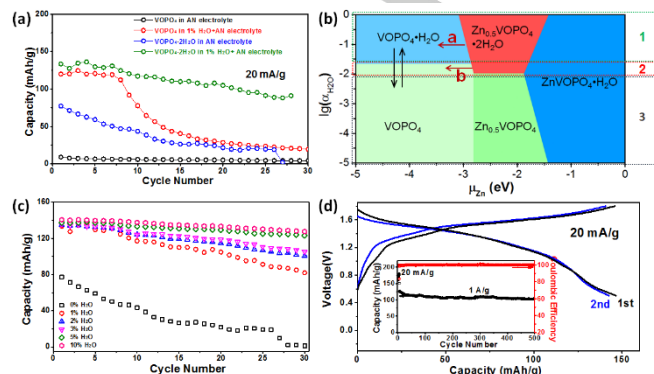


**Figure 4.** (a) The cycling performance of VOPO<sub>4</sub> and VOPO<sub>4</sub>·2H<sub>2</sub>O in different electrolytes. (b) The phase diagram of Zn<sub>x</sub>VOPO<sub>4</sub>·nH<sub>2</sub>O as a function of water activity ( $\alpha_{H_2O}$ ) and Zn chemical potential ( $\mu_{Zn}$ ). (c) The cycling performance of VOPO<sub>4</sub>·2H<sub>2</sub>O in electrolytes with different water contents at 20 mA/g. (d) The electrochemical performance of VOPO<sub>4</sub>·2H<sub>2</sub>O in 4 m Zn(OTf)<sub>2</sub> aqueous electrolyte.

All experimental evidences converge to the conclusion that water-redistribution occurs spontaneously between electrolyte and VOPO<sub>4</sub> and does not rely on the electric field. The sheer driving force behind this process should be the water activity ( $\alpha_{H_2O}$ ) or its concentration gradient in two neighboring materials<sup>[17]</sup>. Given the fact that  $\alpha_{H_2O}$  in the electrolyte depends on the H<sub>2</sub>O concentration that may change with time, and that water uptake for the electrode also depends on  $\alpha_{H_2O}$ , the water concentration equilibrium between electrolyte and electrode should be a key parameter for cycling stability. Figure 4a shows the cycling performance of VOPO<sub>4</sub> and VOPO<sub>4</sub>·2H<sub>2</sub>O in anhydrous and moist electrolytes, respectively. The dehydrated VOPO<sub>4</sub> extracts H<sub>2</sub>O from the moist electrolyte and became electrochemically active, but as expected, the capacity decayed rapidly after only several cycles, because H<sub>2</sub>O diffusion into VOPO<sub>4</sub> would dehydrate the interface and reduces  $\alpha_{H_2O}$  in the electrolyte. Equally, VOPO<sub>4</sub>·2H<sub>2</sub>O showed a persistent capacity fading in the dry electrolyte because the lattice H<sub>2</sub>O kept migrating into the electrolyte, leaving an insufficiently hydrated interface and lattice. In comparison, the optimum capacity retention is demonstrated for VOPO<sub>4</sub>·2H<sub>2</sub>O in the moist electrolyte (Figure S6).

To reveal the influence of  $\alpha_{H_2O}$  during the zincation process of VOPO<sub>4</sub>, the phase diagram of Zn<sub>x</sub>VOPO<sub>4</sub>·nH<sub>2</sub>O as a function of  $\alpha_{H_2O}$  and Zn chemical potential ( $\mu_{Zn}$ ) are calculated using DFT simulations (Figure 4b). The high  $\mu_{Zn}$  refers to a highly zincated Zn<sub>x</sub>VOPO<sub>4</sub>·nH<sub>2</sub>O, while decreasing  $\mu_{Zn}$  corresponds to the de-zincation. In region 1 with  $\alpha_{H_2O}$  above 10<sup>-1</sup>, the reversible zincation process happens between the two hydrated phases through route a. In region 3 with low  $\alpha_{H_2O}$ , the reversible zincation could not

## COMMUNICATION

proceed. In the intermediate region 2 with moderate  $\alpha_{\text{H}_2\text{O}}$ , the four-phase coexistence makes the process rather complicated, where the de-zincation could proceed through route b. As one could predict from the phase diagram, the de-zincation of  $\text{Zn}_{0.5}\text{VOPO}_4 \cdot 2\text{H}_2\text{O}$  along with the release of  $\text{H}_2\text{O}$  into the electrolyte increases  $\alpha_{\text{H}_2\text{O}}$  in the electrolyte. If the increased  $\alpha_{\text{H}_2\text{O}}$  is not sufficiently high to support the hydration of  $\text{VOPO}_4$ , the capacity decay will happen. Therefore, this region should be circumvented to achieve desirable cyclability.

Although the quantitative relation between  $\alpha_{\text{H}_2\text{O}}$  and the  $\text{H}_2\text{O}$  content in the electrolyte needs further investigation, the phase diagram shows that once  $\text{H}_2\text{O}$  content is high enough to maintain the electrochemical process in region 1, a reversible and facile  $\text{Zn}^{2+}$  diffusion could happen, as confirmed by cyclability of  $\text{VOPO}_4 \cdot 2\text{H}_2\text{O}$  in different electrolytes (Figure 4c). When the water content increased from 0 to 5%, the capacity retention improved significantly, although excessive water content above 5% will not further enhance the cycle stability. Certainly,  $\text{VOPO}_4 \cdot 2\text{H}_2\text{O}$  could cycle well in the pure aqueous electrolyte and delivered a discharge capacity of 147 mAh/g (Figure 4d), with excellent cycling stability at a decay rate of 0.027% per cycle at the high rate of 1 A/g. On the other hand, similar cycling stability is achieved by  $\text{VOPO}_4$  (Figure S7), if sufficient time is given to allow the interface as well as the electrode lattice to be fully hydrated. It is noteworthy that even in the aqueous electrolyte the water exchange still happens and the dynamic equilibrium could be easily achieved, as indicated by the reversible structural evolution (Figure S8).

In conclusion, we demonstrate that  $\text{VOPO}_4$  could be utilized as a  $\text{Zn}^{2+}$ -intercalation host, and that  $\text{H}_2\text{O}$  molecule plays a critical role in enabling its electrochemical activity and reversibility. A hydrated electrode/electrolyte interface assists facile  $\text{Zn}^{2+}$  diffusion, while the lattice  $\text{H}_2\text{O}$  dictates  $\text{Zn}^{2+}$ -insertion potential. It is proposed that only  $\text{H}_2\text{O}$  molecules with enough activity could shuttle between the electrolyte and electrode, and a dynamic  $\text{H}_2\text{O}$  equilibrium is eventually established between the the electrode lattice and the electrolyte. To achieve a high cycability,  $\alpha_{\text{H}_2\text{O}}$  should be above  $10^{-1}$ . Although the present work selects  $\text{Zn}^{2+}$  and  $\text{VOPO}_4$  host as candidates of thorough investigation, the fundamental mechanism established herein should universally apply to electrode/electrolyte systems of other bivalent ion chemistries.

## Experimental Section

Experimental Details could be found in the supporting information.

## Acknowledgements

The PIs (KX and CSW) gratefully acknowledge the funding support from DOE ARPA-E (DEAR0000389) and Center of Research on Extreme Batteries (CREB). We also acknowledge the support of the Maryland Nano Center and its NispLab. The NispLab is supported in part by the NSF as a MRSEC Shared Experimental Facility. F.W. was supported by the Oak Ridge Associated Universities (ORAU) through contract W911NF-16-2-0202.

**Keywords:** Aqueous battery • Zn-ion battery • Multivalent battery •  $\text{H}_2\text{O}$  diffusion • Kinetics

- [1] (a) Dunn, H. Kamath, J.-M. Tarascon, *Science* **2011**, 334, 928-935; (b) J. B. Goodenough, K.-S. Park, *J. Am. Chem. Soc.* **2013**, 135, 1167-1176; (c) B. Scrosati, J. Garche, *J. Power Sources* **2010**, 195, 2419-2430.
- [2] (a) D. Larcher, J.-M. Tarascon, *Nat. Chem.* **2015**, 7, 19; (b) J. B. Goodenough, Y. Kim, *Chem. Mater.* **2010**, 22, 587-603; (c) M. Jacoby, *Chem. Eng. News* **2013**, 91, 33-37; (d) M. S. Whittingham, *Chem. Rev.* **2014**, 114, 11414-11443.
- [3] (a) J. W. Choi, D. Aurbach, *Nature Reviews Materials* **2016**, 1, 16013; (b) P. Canepa, G. Sai Gautam, D. C. Hannah, R. Malik, M. Liu, K. G. Gallagher, K. A. Persson, G. Ceder, *Chem. Rev.* **2017**, 117, 4287-4341; (c) M. Wang, C. Jiang, S. Zhang, X. Song, Y. Tang, H.-M. Cheng, *Nat. Chem.* **2018**, 1; (d) S.-B. Son, T. Gao, S. P. Harvey, K. X. Steirer, A. Stokes, A. Norman, C. Wang, A. Cresce, K. Xu, C. Ban, *Nat. Chem.* **2018**, 10, 532.
- [4] (a) Z. Rong, R. Malik, P. Canepa, G. Sai Gautam, M. Liu, A. Jain, K. Persson, G. Ceder, *Chem. Mater.* **2015**, 27, 6016-6021; (b) G. Sai Gautam, P. Canepa, W. D. Richards, R. Malik, G. Ceder, *Nano Lett.* **2016**, 16, 2426-2431; (c) M. S. Chae, J. W. Heo, S. C. Lim, S. T. Hong, *Inorg. Chem.* **2016**, 55, 3294-3301; (d) X. Sun, V. Duffort, B. L. Mehdi, N. D. Browning, L. F. Nazar, *Chem. Mater.* **2016**, 28, 534-542.
- [5] (a) K. W. Nam, S. Kim, S. Lee, M. Salama, I. Shterenberg, Y. Gofer, J. S. Kim, E. Yang, C. S. Park, J. S. Kim, S. S. Lee, W. S. Chang, S. G. Doo, Y. N. Jo, Y. Jung, D. Aurbach, J. W. Choi, *Nano Lett.* **2015**, 15, 4071-4079; (b) H. J. Lee, J. Shin, J. W. Choi, *Adv. Mater.* **2018**, 1705851.
- [6] D. Kundu, S. H. Vajargah, L. Wan, B. Adams, D. Prendergast, L. F. Nazar, *Energy Environ. Sci.* **2018**.
- [7] K. Amann-Winkel, M.-C. Bellissent-Funel, L. E. Bove, T. Loerting, A. Nilsson, A. Paciaroni, D. Schlesinger, L. Skinner, *Chem. Rev.* **2016**, 116, 7570-7589.
- [8] (a) D. Kundu, B. D. Adams, V. Duffort, S. H. Vajargah, L. F. Nazar, *Nature Energy* **2016**, 1, 16119; (b) H. Pan, Y. Shao, P. Yan, Y. Cheng, K. S. Han, Z. Nie, C. Wang, J. Yang, X. Li, P. Bhattacharya, K. T. Mueller, J. Liu, *Nature Energy* **2016**, 1, 16039; (c) J. F. Parker, C. N. Chervin, I. R. Pala, M. Machler, M. F. Burz, J. W. Long, D. R. Rolison, *Science* **2017**, 356, 415-418; (d) S. Selverston, R. F. Savinell, J. S. Wainright, *J. Electrochem. Soc.* **2017**, 164, A1069-A1075;
- [9] M. S. Chae, J. W. Heo, H. H. Kwak, H. Lee, S.-T. Hong, *J. Power Sources* **2017**, 337, 204-211.
- [10] (a) Y. Zhu, L. Peng, D. Chen, G. Yu, *Nano Lett.* **2016**, 16, 742-747; (b) C. Wu, X. Lu, L. Peng, K. Xu, X. Peng, J. Huang, G. Yu, Y. Xie, *Nat Commun* **2013**, 4, 2431.
- [11] R. Gautier, N. Audebrand, E. Furet, R. Gautier, E. L. Fur, *Inorg. Chem.* **2011**, 50, 4378-4383.
- [12] G. He, W. H. Kan, A. Manthiram, *Chem. Mater.* **2016**, 28, 682-688.
- [13] L. Scatena, M. Brown, G. Richmond, *Science* **2001**, 292, 908-912.
- [14] (a) A. Narten, W. Thiessen, L. Blum, *Science* **1982**, 217, 1033-1034; (b) D. S. Charles, M. Feyngenson, K. Page, J. Neuefeind, W. Xu, X. Teng, *Nat Commun* **2017**, 8, 15520.
- [15] (a) N. Zhang, F. Cheng, J. Liu, L. Wang, X. Long, X. Liu, F. Li, J. Chen, *Nat. Commun.* **2017**, 8, 405; (b) L. W. Juang, P. J. Kollmeyer, T. M. Jahns, R. D. Lorenz, *IEEE Trans. Ind. Appl.* **2013**, 49, 1480-1488.

COMMUNICATION

---

- [16] J. Zheng, Y. Hou, Y. Duan, X. Song, Y. Wei, T. Liu, J. Hu, H. Guo, Z. Zhuo, L. Liu, *Nano Lett.* **2015**, *15*, 6102-6109.
- [17] S. Römhild, M. Hedenqvist, G. Bergman, *Polymer Engineering & Science* **2012**, *52*, 718-724.

WILEY-VCH

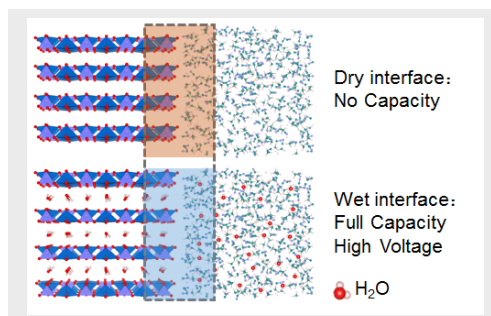
Accepted Manuscript

## COMMUNICATION

## Entry for the Table of Contents

## COMMUNICATION

H<sub>2</sub>O at the electrolyte/electrode interface plays the key role in assisting Zn<sup>2+</sup> diffusion from electrolyte to the bulk surface, while H<sub>2</sub>O in the lattice structure alters the working potential. A dynamic equilibrium between bulk electrode and electrolyte is eventually established for the H<sub>2</sub>O transports during the charge/discharge cycles, with the water activity being the key parameter determining the direction of water movement and the cycling stability.



Fei Wang,[a],[b] Wei Sun, [a] Zulipiya Shadike, [c] Enyuan Hu, [c] Xiao Ji,[a] Tao Gao, [a] Xiao-Qing Yang, [c] Kang Xu\* [b] and Chunsheng Wang\* [a]

Page No. – Page No.

**How Water Accelerates Bivalent Ion Diffusion**

Accepted Manuscript